Genes to Cells

In vivo tracking of histone H3 lysine 9 acetylation in *Xenopus laevis* during tail regeneration

Miyuki Suzuki[1], Chiyo Takagi[2], Shinichirou Miura[3], Yuto Sakane[1], Makoto Suzuki[2,4], Tetsushi Sakuma[1], Naoaki Sakamoto[1], Tetsuya Endo[3], Yasuhiro Kamei[4,5], Yuko Sato[6], Hiroshi Kimura[6], Takashi Yamamoto[1], Naoto Ueno[2,4] and Ken-ichi T. Suzuki[1]*

[1]*Department of Mathematical and Life Sciences, Graduate School of Science, Hiroshima University, 1-3-1 Kagamiyama, Higashihiroshima 739-8526, Hiroshima, Japan*
[2]*Division of Morphogenesis, National Institute for Basic Biology, 38 Nishigonaka, Myodaiji, Okazaki 444-8585, Aichi, Japan*
[3]*Division of Liberal Arts and Sciences, Aichi Gakuin University, 12 Araike, Iwasaki, Nissin 470-0195, Aichi, Japan*
[4]*Department of Basic Biology, School of Life Science, the Graduate University for Advanced Studies (SOKENDAI), 38 Nishigonaka, Myodaiji, Okazaki 445-8585, Aichi, Japan*
[5]*Spectrography and Bioimaging Facility, National Institute for Basic Biology, 38 Nishigonaka, Myodaiji, Okazaki 444-8585, Aichi, Japan*
[6]*Department of Biological Sciences, Graduate School of Bioscience and Biotechnology, Tokyo Institute of Technology, Yokohama 226-8501, Japan*

***Xenopus laevis* tadpoles can completely regenerate their appendages, such as tail and limbs, and therefore provide a unique model to decipher the molecular mechanisms of organ regeneration in vertebrates. Epigenetic modifications are likely to be involved in this remarkable regeneration capacity, but they remain largely unknown. To examine the involvement of histone modification during organ regeneration, we generated transgenic *X. laevis* ubiquitously expressing a fluorescent modification-specific intracellular antibody (Mintbody) that is able to track histone H3 lysine 9 acetylation (H3K9ac) *in vivo* through nuclear enhanced green fluorescent protein (EGFP) fluorescence. In embryos ubiquitously expressing H3K9ac-Mintbody, robust fluorescence was observed in the nuclei of somites. Interestingly, H3K9ac-Mintbody signals predominantly accumulated in nuclei of regenerating notochord at 24 h postamputation following activation of reactive oxygen species (ROS). Moreover, apocynin (APO), an inhibitor of ROS production, attenuated H3K9ac-Mintbody signals in regenerating notochord. Our results suggest that ROS production is involved in acetylation of H3K9 in regenerating notochord at the onset of tail regeneration. We also show this transgenic *Xenopus* to be a useful tool to investigate epigenetic modification, not only in organogenesis but also in organ regeneration.**

Introduction

Xenopus laevis larvae can functionally and morphologically regenerate their organs, such as limb, tail and brain; however, tadpoles lose regeneration competence as metamorphosis progresses and froglets show defective limb regeneration (Dent 1962; reviewed by Suzuki *et al.* 2006) and completely fail to regenerate their brain (Yoshino & Tochinai 2004; reviewed by Endo *et al.* 2007). Appendage regeneration, in particular forelimb and hindlimb regeneration, have been extensively studied to decipher the molecular mechanisms underlying the remarkable capability of organ regeneration in *Xenopus* (reviewed by Suzuki *et al.* 2006; Beck *et al.* 2009; Yakushiji *et al.* 2009).

Recently, *Xenopus* tadpole tail regeneration has also emerged as a new model for studying the molecular basis of appendage regeneration in vertebrates because the tail has a simple structure and is composed mainly of spinal cord, notochord, muscle and skin (reviewed by Mochii *et al.* 2007; Slack *et al.* 2008; Tseng & Levin 2008; Beck *et al.* 2009). Slack

Communicated by: Masayuki Miura
**Correspondence:* suzuk107@hiroshima-u.ac.jp and suzuken107@gmail.com

DOI: 10.1111/gtc.12349

and colleagues have extensively studied multiple signaling pathways that are required for tail regeneration, including bone morphogenetic protein (Bmp) (Beck *et al.* 2003, 2006), Notch (Beck *et al.* 2003), fibroblast growth factor (Fgf) and Wnt pathways (Lin & Slack 2008; Lin *et al.* 2012). Moreover, Taniguchi *et al.* (2014) have also showed the requirement for Hedgehog signaling, a key factor for organ development, in tail regeneration. Reactivation of these molecular pathways might make it possible to recapitulate the developmental process in tail regeneration after organogenesis; however, it remains unclear how reactivation of these pathways and genes is controlled.

Involvement of epigenetic regulation in amphibian regeneration has been investigated owing to its importance in general gene regulation; CpG methylation and histone acetylation are two major epigenetic modifications that control gene inactivation and activation, respectively. For instance, sonic hedgehog (*shh*) is thought to be required for complete limb regeneration in *Xenopus* (Endo *et al.* 1997, 2000). Intriguingly, reactivation of *shh* is suppressed and its limb-specific enhancer region (MFCS1) is hypermethylated in the blastema of froglets but not tadpoles (Yakushiji *et al.* 2007). Moreover, inhibition of histone deacetylases (HDACs) that generally induce gene inactivation causes failure of tail and hindlimb regeneration (Tseng *et al.* 2011; Taylor & Beck 2012). Involvement of epigenetic regulation in organ regeneration was also reported in invertebrates. In cricket leg regeneration, knockdown of *enhancer of zeste* (*E*(*z*)) and *Utx* causes down- and up-regulation of histone H3K27 methylation (H3K27me), respectively (Hamada *et al.* 2015). The perturbation of H3K27me results in abnormal leg regeneration (Hamada *et al.* 2015).

Epigenetic regulation in organ regeneration is an issue to be solved; however, spatiotemporal and cell-specific changes of epigenetic modifications in regenerating organs have not been well examined because of a lack of molecular methods for analyzing epigenetic modifications *in vivo*. Recently, Sato *et al.* (2013) established a technique to track *in vivo* acetylation of lysine 9 in histone H3 (H3K9ac) using a fluorescent protein, H3K9ac-Mintbody (modification-specific intracellular antibody) based on antigen–antibody interaction. H3K9ac-Mintbody consists of a single-chain variable fragment (scFv) antibody against H3K9ac and enhanced green fluorescent protein (EGFP). H3K9ac-Mintbody specifically binds to H3K9ac and consequently accumulates in nuclei. The dynamics of acetylation and active chromatin status can therefore be observed *in vivo* as intensity of nuclear EGFP fluorescence. In fruit fly and zebrafish, studies of transgenic embryos stably expressing H3K9ac-Mintbody have showed dynamic changes in H3K9ac levels during embryogenesis (Sato *et al.* 2013).

In the present study, we generated transgenic *X. laevis* ubiquitously expressing H3K9ac-Mintbody to track H3K9ac *in vivo*. Transgenic embryos showed a unique spatiotemporal nuclear fluorescence pattern that revealed the dynamics of H3K9ac in early embryogenesis and tail regeneration. We also show correlation between reactive oxygen species (ROS) production and H3K9ac at the onset of tail regeneration.

Results

Tracking H3K9ac dynamics during early embryogenesis

First, to examine whether H3K9ac-Mintbody can track an active histone mark, H3K9ac, *in vivo* in *X. laevis*, we injected Mintbody mRNA into fertilized eggs and observed its EGFP fluorescence signal. Although injected mRNA should uniformly disperse throughout the whole egg, Mintbody mRNA-injected embryos showed a unique fluorescence pattern (Fig. 1A,B): Fluorescence signal is detectable in somites at NF stage 32, and was sustained there until NF stage 41. However, the intensity of the Mintbody signal declined as development progressed, and finally became undetectable by 10 days after fertilization. Thus, Mintbody signal from injected mRNA could no longer track H3K9ac after the swimming tadpole stage.

Next, to track H3K9ac *in vivo* throughout early embryogenesis and postembryonic events such as regeneration, we made transgenic *X. laevis* ubiquitously expressing H3K9ac-Mintbody using the microhomology-mediated end-joining (MMEJ)-dependent knock-in technique (Nakade *et al.* 2014). This method is explained briefly as follows. Transcription activator-like effector nucleases (TALENs) mRNAs targeting *tyr* exon 1 (*xltyr*TALENs) and donor vector containing CMV promoter/Mintbody cDNA were co-injected into fertilized eggs. The donor vector also had *xltyr*TALENs target sites that contained a modified spacer sequence, in which the anterior and posterior halves are switched. *xltyr*TALENs induce double-strand breaks in their target loci and linearize the donor vector with the modified microhomologous sequences, and consequently, the CMV promoter/Mintbody

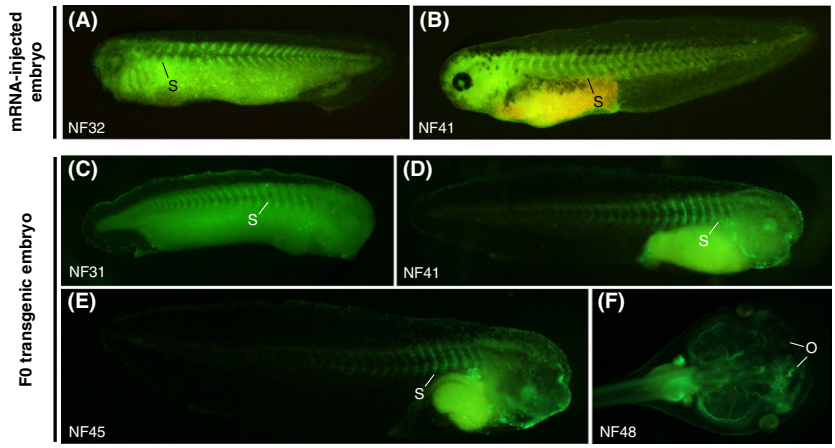

Figure 1 H3K9ac-Mintbody enhanced green fluorescent protein (EGFP) fluorescence pattern during early embryogenesis. (A, B) EGFP fluorescence pattern of Mintbody mRNA-injected embryos during early embryogenesis. EGFP Fluorescence images at NF stage 32 (A) and 41 (B) were captured using a fluorescence stereomicroscope. S, somite. (C–F) CMV:Mintbody F0 embryos during early embryogenesis. EGFP fluorescence images at NF stage 31 (C), 41 (D), 45 (E) and 48 (F). S, somite; O, olfactory epithelium.

cDNA was integrated into the *tyr* locus via MMEJ repair (Fig. S1A in Supporting Information). Successful transgenic phenotypes were characterized by both albinism and robust fluorescence signal in the nuclei of somites, in a similar pattern to that seen in mRNA-injected embryos (Fig. 1C–F). Mintbody signal was ubiquitously observed in founder (F0) embryos at the swimming stage (Fig. 1E,F). Approximately 30% of embryos exhibited normal development possessing EGFP fluorescence in somites (Fig. S1B,C in Supporting Information).

Tracking H3K9ac dynamics during tail regeneration

To investigate H3K9ac dynamics *in vivo* during organ regeneration, we observed amputated tails of CMV:Mintbody F0 embryos at NF41 (Fig. 2A–G). Although the nuclear fluorescence signal was faint just after tail amputation, it became strong and its level reached a peak in regenerating notochord at 1 or 2 days postamputation (dpa) (Fig. 2C–E,I). Immunohistochemical analysis confirmed that the fluorescence signals were clearly enriched in nuclei of regenerating notochord (Fig. 2H). Besides, Mintbody signal was seen in neural ampulla (Fig. 2D′). In five independent experiments, 26 of 32 (81%) F0 embryos showed strong nuclear Mintbody signal in regenerating notochord at 1 dpa (Table 1). To confirm the reproducibility of the results, we also generated Mintbody F0 embryos using more ubiquitous promoter, *elongation factor 1-alpha* (EF1a) promoter, and the I-SceI transgenic method (Ogino *et al.* 2006). In good agreement with results from the CMV:Mintbody F0 embryos, a similar fluorescence pattern during embryogenesis and in the regenerating tail at 1 dpa was observed in EF1a:Mintbody F0 embryos (Fig. S2 in Supporting Information). Moreover, we observed similar patterns of Mintbody signal in the notochord of CMV:Mintbody F1 embryos at 1 dpa from F0 generated by a restriction enzyme-mediated integration (REMI) method (Fig. S3 in Supporting Information). Besides, Mintbody signal was seen in neural ampulla and wound epithelium (Fig. S3H in Supporting Information). In F1 growing tadpoles, the nuclear fluorescence signal was not observed just after tail amputation. It became strong and its level reached a peak in regenerating notochord at 1 or 2 dpa as with the results of embryos (Fig. S3I–L′ in Supporting Information). These data suggest that H3K9ac induction in regenerating tail occurs in common between embryogenesis and the later tadpole stage.

To examine whether the Mintbody signal faithfully tracked the dynamics of histone acetylation *in vivo*, we treated F1 transgenic embryos with TSA, an inhibitor of HDACs. As expected, enhancement of Mintbody signal was seen in all TSA-treated embryos but not in solvent-treated embryos ($n = 3$ each; Fig. S4 in Supporting Information) suggesting that CMV:Mintbody embryos were able to track H3K9ac dynamics *in vivo*. It is,

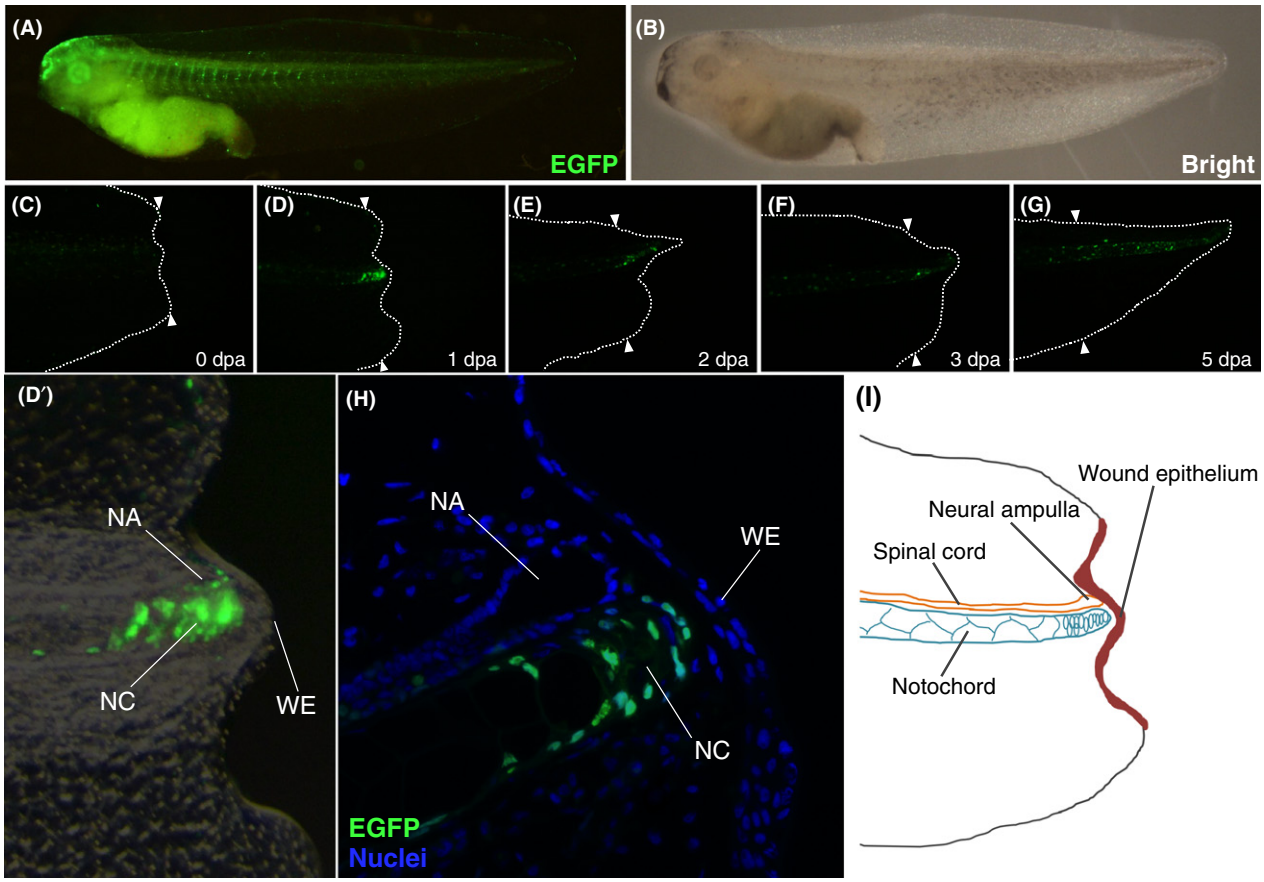

Figure 2 Enhanced green fluorescent protein (EGFP) fluorescence pattern of CMV:H3K9ac-Mintbody F0 embryos during tail regeneration. EGFP fluorescence (A) and bright-field (B) images of a representative embryo just before tail amputation at NF stage 41. Continuous EGFP fluorescence images at 0 dpa (C), 1 dpa (D), 2 dpa (E), 3 dpa (F) and 5 dpa (G). Dotted lines trace the shapes of tails. Arrowheads indicate amputation sites. Dorsal side is oriented at the top of each panel. (D′) Merged EGFP fluorescence and bright-field images of (D), high magnification. (H) Localization and tissue distribution of Mintbody in the regenerating tail. Immunohistochemistry was carried out using anti-EGFP-antibody (green) in the sagittal section of an F0 embryo at 1 dpa. Nuclei were counterstained with DAPI (blue). Dorsal side is oriented at the top of the panel. Note that nuclear accumulation of Mintbody is dominantly seen in regenerating notochord. NC, notochord; NA, neural ampulla; WE, wound epithelium. (I) A schematic illustration of regeneration bud during *Xenopus* tail regeneration at 1 dpa in lateral view. Dorsal side is oriented at the top. At 1–2 dpa, regenerating notochord has a bullet-shaped structure.

however, important to validate the effect of TSA on Mintbody signal using different F1 transgenic line in a future study.

To trace the notochord cells showing a strong Mintbody signal, we carried out time-course observation of tail regeneration in F0 embryos (Fig. 3). Strong Mintbody signals appeared in the notochord proximal region (curly brackets in Fig. 3) and regenerating notochord (square brackets in Fig. 3) by 25 h postamputation (hpa). Interestingly, the proximal notochord cells remained in this position during regeneration, whereas the regenerating notochord cells migrated from the amputation site to the tip of the tail to reconstruct the notochord. We also confirmed this phenomenon in F1 embryos (Table 1; Fig. S5 in Supporting Information).

ROS inhibition impairs the increase of H3K9ac during tail regeneration

As described above, the increase of Mintbody signal occurs in regenerating notochord at an early phase of regeneration. To further show early events in tail regeneration, we focused on the involvement of

Table 1 Increases of H3K9ac-Mintbody signal in the regenerating notochord

	Positive	Negative
F0 embryos generated by TALEN-mediated transgenesis	26/32 (81%)	6/32 (19%)
F1 embryos generated by REMI transgenesis	28/28 (100%)	0/28 (0%)

We examined increases of Mintbody signal in regenerating notochord of F0 and F1 embryos at 1 dpa. F0 and F1 embryos were generated by TALEN-mediated transgenesis and REMI transgenesis, respectively. The data were collected from five independent experiments for F0 embryos and from two independent experiments for F1 embryos. TALEN, transcription activator-like effector nucleases; REMI, restriction enzyme-mediated integration.

ROS production in the increase of H3K9ac levels in tail regeneration. ROS are produced immediately after amputation and their inhibition impairs tail regeneration in *Xenopus* (Love *et al.* 2013). A time-course observation of ROS production using H2DCFDA showed that ROS production occurred at the tail amputation site at 1 hpa and was sustained until 6 hpa or later (Fig. 4), raising the possibility that ROS production precedes H3K9ac in tail regeneration.

To examine whether ROS signaling is involved in increased H3K9ac levels, CMV:Mintbody F1 embryos were treated with APO, an NADH oxidase inhibitor. We first determined the APO concentration that was sufficient to impair tail regeneration; most 1 mM APO-treated embryos failed to regenerate tail (Fig. S6 in Supporting Information). Dimethyl sulfoxide (DMSO) treatment did not affect the increase of Mintbody signal in the notochord after amputation, whereas APO treatment clearly blocked the increase in 42 of 47 embryos at 1 dpa (Fig. 5). Unexpectedly, increase of Mintbody signal was observed in the wound epithelium in most APO-treated embryos (Table S2 in Supporting Information). The reproducibility of this phenomenon was confirmed by two independent experiments using embryos from three transgenic F0 parents.

Discussion

Epigenetic regulation by DNA methylation and histone modification is likely to be involved in the control of the recapitulation of developmental processes during amphibian regeneration (Yakushiji *et al.* 2007; Hayashi *et al.* 2015). However, thus far, there has been no means for the *in vivo* analysis of the dynamics of epigenetic modifications in amphibian regeneration. To address this, we show here that H3K9ac-Mintbody transgenic *Xenopus* can track H3K9ac dynamics *in vivo* during tail regeneration.

H3K9ac dynamics can be tracked *in vivo* in Mintbody transgenic *Xenopus*

Mintbody transgenic embryos showed a unique fluorescence pattern during early embryogenesis. Although Mintbody mRNA was ubiquitously expressed, its fluorescence signal was distinctly observed in somite nuclei throughout early embryogenesis. Somite nuclei showing robust Mintbody signal may possess unique chromatin dynamics or nuclear architecture during early embryogenesis. In addition, TSA, a well-known HDAC inhibitor, enhanced the Mintbody signal in the transgenic embryos, indicating that Mintbody has the ability to track H3K9ac dynamics *in vivo* in *X. laevis*, as it does in fruit fly and zebrafish (Sato *et al.* 2013).

Histone acetylation in tail regeneration

Previously, it was shown that treatment with HDAC inhibitors, valproic acid (VPA) and TSA (Tseng *et al.* 2011), or TSA only (Taylor & Beck 2012), impairs tail regeneration. Complete inhibition of tail regeneration requires treatment with VPA by 48 hpa. Indeed, significant changes in H4 acetylation level do not occur in the regenerating tail until at least 24 hpa (Tseng *et al.* 2011), whereas Mintbody transgenic animals showed a clear increase of H3K9ac in regenerating notochord from 16 to 24 hpa. Consistent with these findings, H3 and H4 acetylation have opposite functions for nucleosome reconstitution and chromatin remodeling (Kurdistani *et al.* 2004; Agricola *et al.* 2006; Gansen *et al.* 2015). Acetylation of H3 enhances the opening of the DNA ends and nucleosome disassembly during transcription, whereas, in contrast, acetylation of H4 tends to maintain stable chromatin states. These reports support the hypothesis that bivalent hypoacetylated H4 and hyperacetylated H3 synergistically promote an increase of DNA accessibility at regeneration-related gene loci and consequently reactivate their transcription during tail regeneration.

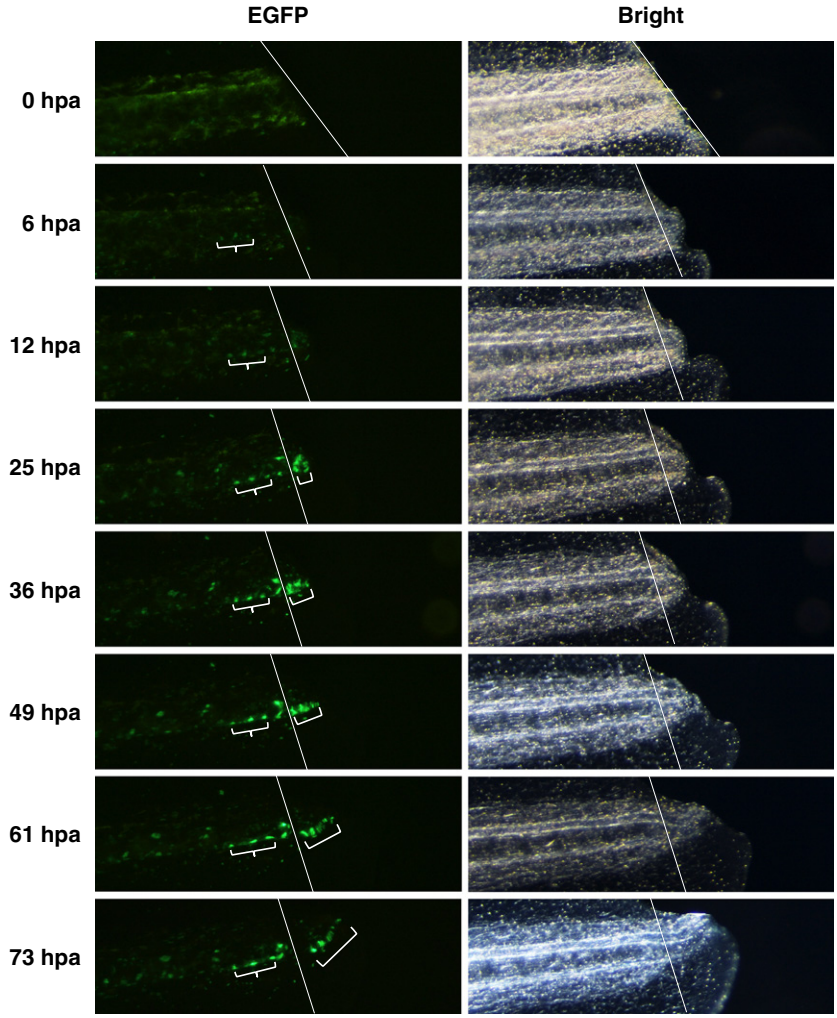

Figure 3 Regenerating notochord cells possessing robust H3K9ac-Mintbody signals migrate and reconstruct notochord. Continuous images of tail regeneration were captured from just after amputation to 73 hpa at the indicated time. Straight lines indicate the amputation site. Curly and square brackets show the proximal notochord and regenerating notochord cells, respectively. Left and right panels show Enhanced green fluorescent protein fluorescence and bright-field images at each indicated time, respectively. Dorsal side is oriented at the top of each panel.

Possible role of notochord H3K9ac-positive cells during tail regeneration

Notochord is thought to be a vital tissue in *Xenopus* tail regeneration because *shh*, an essential factor for appendage formation (St-Jacques *et al.* 1998; Kraus *et al.* 2001), is activated there. Indeed, cyclopamine, a chemical inhibitor of Hedgehog signaling, impairs tail regeneration in *X. laevis* (Taniguchi *et al.* 2014). Interestingly, Mintbody signal increased in the regenerating notochord where *shh* is also activated. Robust nuclear fluorescence signal was observed in the regenerating notochord at 1 dpa, and then, cells showing a high level of H3K9ac entered into the regenerating notochord. Moreover, *fgf20* and Wnt signaling also appear to be expressed or activated in regenerating notochord (Love *et al.* 2013). From these observations, we speculate that H3K9ac contributes to reactivation of regeneration-related genes in regenerating notochord and constitute a signaling center to orchestrate tail formation.

Our observations also provided insight into cell lineage during tail regeneration. We observed that regenerating notochord cells showing strong nuclear

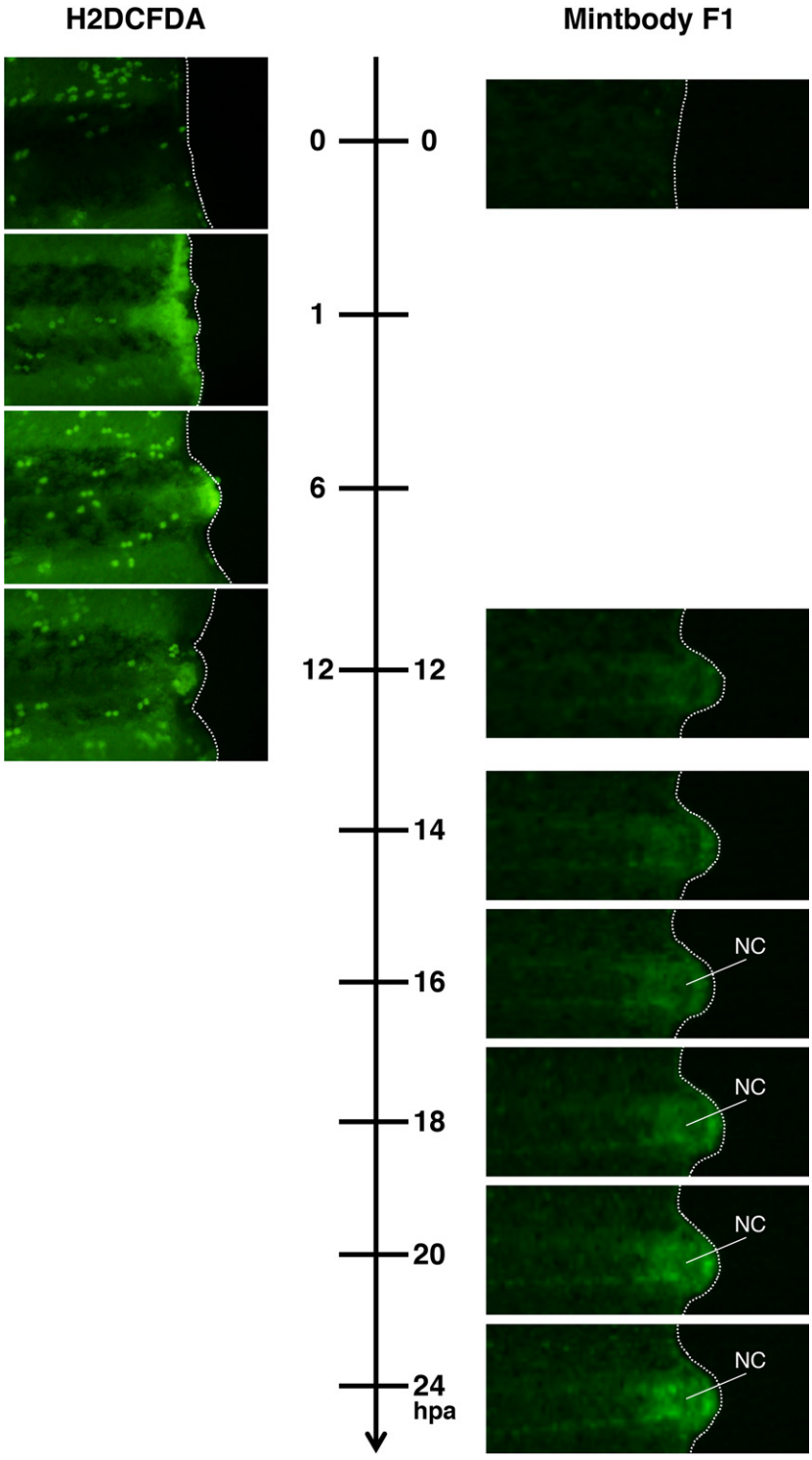

Figure 4 Reactive oxygen species (ROS) production and the increase of H3K9ac-Mintbody signal at the onset of tail regeneration. To visualize ROS production, wild-type embryos were exposed to H2DCFDA 2 h before observation at each indicated time. Mintbody signals in F1 embryos were observed from 0 to 24 hpa at each time point. Dotted lines trace the shapes of tails. NC, notochord. Dorsal side is oriented at the top of each panel.

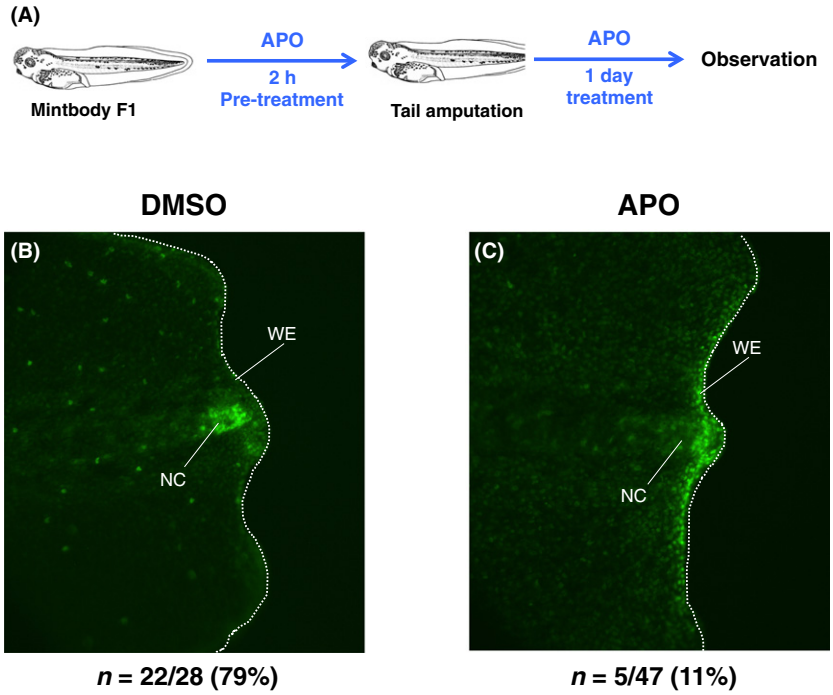

Figure 5 Reactive oxygen species (ROS) inhibition impairs the increase of H3K9ac-Mintbody signal in tail regeneration. (A) A scheme of ROS inhibition in tail regeneration. F1 embryos at NF stage 41 were pre-treated with apocynin (APO), an inhibitor of ROS production, for 2 h before amputation; then, tails were amputated. Mintbody signal was observed at 1 dpa. *Xenopus* images from Nieuwkoop & Faber (1994) were modified. (B, C) Representative images of dimethyl sulfoxide (DMSO)- and APO-treated embryos. Mintbody signals were seen in the notochord of control DMSO-treated embryos (B; $n = 22$ positive in notochord/28 total, 79%), whereas no or faint signal was seen in the notochord of APO-treated embryos (C; $n = 5$ positive in notochord/47 total, 11%). The data were obtained from two independent experiments using three different F0 parents. Dotted lines trace the shapes of tails. NC, notochord; WE, wound epithelium. Dorsal side is oriented at the top of each panel.

EGFP fluorescence appear to migrate and rebuild the notochord itself during tail regeneration. This observation is in good agreement with the following common view. Although a blastema (defined as a mass of dedifferentiated proliferating cells) appears in regenerating appendages including limbs, it is not observed in regenerating tail. In other words, each cell in muscle, spinal cord and notochord retains its initial cell fate in regenerating tail (Gargioli & Slack 2004; Chen *et al.* 2006; Mochii *et al.* 2007).

Involvement of ROS production in the increase of H3K9ac levels during tail regeneration

The inhibition of ROS signaling by chemical compounds impairs tail regeneration (Love *et al.* 2013). In this study, we observed that ROS production occurred immediately after tail amputation before the increase in H3K9ac levels. Intriguingly, inhibition of ROS production by APO attenuated the increase of H3K9ac levels in regenerating notochord at 1 dpa, suggesting that amputation-induced ROS signaling precedes the acetylation of H3K9 (Fig. 6). Pre-treatment with ROS inhibitors, such as APO, significantly reduces ethanol-induced H3K9ac in rat hepatocytes (Choudhury *et al.* 2010), supporting the involvement of ROS in increasing H3K9ac levels.

Beck *et al.* (2003) first reported that regeneration capability of tail is drastically decreased at NF stage 45–47, so-called the refractory period. Interestingly, activation of immune response is involved in loss of tail regeneration during the refractory period (Fukazawa *et al.* 2009; Naora *et al.* 2013). ROS induction occurs before the accumulation of inflammatory cells (Love *et al.* 2013); therefore, H3K9ac in the notochord would not be directly induced by immune response at the early phase of tail regeneration.

Unexpectedly, inhibition of ROS production caused an increase of Mintbody signal in wound

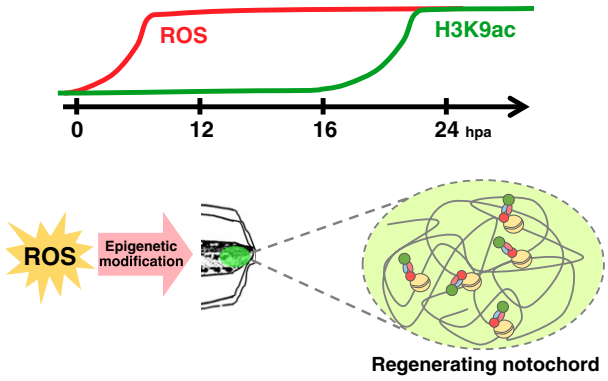

Figure 6 Schematic model of reactive oxygen species (ROS) production and H3K9ac modification at the onset of tail regeneration. After amputation, ROS are immediately produced near the amputation site and its production is sustained during tail regeneration. Acetylation of H3K9 is subsequently induced at the amputation site, in particular, in the notochord from 16 to 24 hpa.

epithelium. In limb regeneration, wound epithelium eventually thickens into regeneration-permissive wound epithelium, called apical epithelial cap (AEC) (Satoh *et al.* 2008; Stocum 2011), and formation and elongation of a blastema occur under the influence of AEC. Presumably it is also necessary in tail regeneration. Besides, mitochondrial ROS facilitates epidermal differentiation and hair follicle development via beta-catenin activation and Notch signaling in mouse (Hamanaka *et al.* 2013). Therefore, we speculate that hyperacetylation of H3K9 by low level of ROS blocks wound epithelium to differentiate into AEC via inhibition of Wnt signaling, which results in failure of tail regeneration. Actually, hyperacetylation of H4 in wound epithelium seems to block tail regeneration in *Xenopus* (Tseng *et al.* 2011). We are currently exploring this question.

Multiple signaling pathways are reported to be crucial for tail regeneration; Hedgehog signaling (Taniguchi *et al.* 2014), Wnt and Fgf pathways (Lin & Slack 2008; Love *et al.* 2011, 2013; Lin *et al.* 2012). ROS inhibition also decreases the activation of Wnt signaling and *fgf20* expression during tail regeneration (Love *et al.* 2013; Chen *et al.* 2014). Therefore, given that H3K9ac is generally involved in gene activation, we speculate that ROS signaling facilitates the reactivation of *shh*, *wnt* and *fgf* genes through the increase of H3K9ac levels in notochord at the onset of tail regeneration. Involvement of ROS in regeneration has also been reported in zebrafish and planaria (Gauron *et al.* 2013; Pirotte *et al.* 2015); therefore, the relationship between ROS and epigenetic modifications may be a conserved principle of regeneration in various organisms.

Histone modifications in *Xenopus* regeneration

In *X. laevis*, the mechanisms underlying loss of regeneration capability during metamorphosis (Dent 1962) or the refractory period (Beck *et al.* 2003; Fukazawa *et al.* 2009) are still unsolved riddles. A key to unravel the riddles is further comprehension of histone modifications in organ regeneration. For example, Hayashi *et al.* (2015) reported that an inhibitor of histone methyltransferase EZH2 that catalyzes H3K27 trimethylation reduces limb regeneration in *Xenopus* tadpole, suggesting that inactive chromatin marks are also involved in organ regeneration. They also reported that H3K27 and H3K4 trimethylation are unchanged in limb bud regeneration using chromatin immunoprecipitation sequencing (ChIP-Seq). Further analysis of histone modifications in the refractory period, metamorphosis and adulthood is required for understanding of decrease of regeneration capability throughout ontogeny using useful tools such as ChIP-Seq and Mintbody transgenic *Xenopus*.

Experimental procedures

Animal manipulation and microinjection

Xenopus laevis adults were purchased from Hamamatsu Seibutsu Kyouzai, Japan. Fertilized eggs were obtained from sexually mature females and males by injecting human chorionic gonadotropin (Aska Pharmaceutical). To provide testes for *in vitro* fertilization, males were deeply anesthetized and killed by injecting 400 μL of 10% MS-222 (Tricaine; Sigma). Eggs were dejellied using 2% cysteine in 0.1× Marc's modified ringer (MMR) adjusted to pH 7.8 with NaOH, washed with 0.1× MMR and transferred into 5% Ficoll (Sigma-Aldrich) in 0.3× MMR. Microinjection was carried out using a Nanoject II (Drummond), and injected embryos were reared in 0.1× MMR containing 50 μg/mL gentamicin at 18 °C (Suzuki *et al.* 2013). Developmental staging was carried out according to Nieuwkoop and Faber (NF stage; Nieuwkoop & Faber 1994). For anesthetic before tail amputation, MS-222 was used at the final concentration of 0.01%–0.05%. To confirm changes in levels of H3K9ac, Mintbody transgenic embryos at NF stage 41 were individually incubated in 5 mL of 0.1× MMR containing 100 nM trichostatin A (TSA; Calbiochem) in a 6-well plate for 45 h. TSA was dissolved in 100% EtOH at a stock concentration of 100 μM. This TSA-containing MMR was changed every 24 h. Animal rearing and treatment were approved and carried out to according to the Hiroshima University and National Institute for Basic Biology guidelines for the use and care of experimental animals.

mRNA injection

Amino acid sequences of histone H3 between human and *X. laevis* are 100% identical; therefore, H3K9ac-Mintbody must recognize *Xenopus* H3K9ac. Mintbody cDNA was PCR amplified from pEGFP-N2/H3K9ac-Mintbody and subcloned into the BamHI and XbaI sites of pCS2+ (Turner & Weintraub 1994; Sato *et al.* 2013). mRNA was transcribed *in vitro* using an mMESSAGE mMACHINE SP6 Transcription Kit (Life Technologies) from linearized pCS2+/Mintbody. Five hundred pg of Mintbody mRNA was injected into fertilized eggs at the one-cell stage.

Transgenesis

Platinum TALENs were designed to target *X. laevis tyr* exon 1 (*xltyr*TALEN) (Previously described in Sakuma *et al.* 2013; Sakane *et al.* 2014). *xltyr*TALEN mRNA was transcribed *in vitro* using an mMESSAGE mMACHINE T7 ULTRA Transcription Kit (Life Technologies). A modified *xltyr*TALEN recognition site for target integration (TACTT CTTGCTGCACTGGGAATTCAGAAACATGAGCTCAC GGGAGATGAGA) was added upstream of the CMV promoter of pEGFP-N2/H3K9ac-Mintbody (Sato *et al.* 2013) or pCS2+/Mintbody using inverse PCR with specific primer sets (Table S1 in Supporting Information) and the resultant plasmids were used as a donor vector. Approximately 250 pg of each right and left *xltyr*TALEN mRNA and 100 pg of donor vector were co-injected into eggs at the one-cell stage. This TALEN-based transgenic method was based on Nakade *et al.* (2014; Fig. S1 in Supporting Information). For I-SceI transgenesis, IS-pXeX was used as the donor plasmid (Johnson & Krieg 1994; a kind gift from Dr. Haruki Ochi and NBRP '*Xenopus tropicalis*'). Mintbody cDNA was subcloned into BamHI and XbaI sites of IS-pXeX. Transgenesis was carried out according to Ogino *et al.* (2006). The REMI transgenic method was carried out according to Kroll & Amaya (1996) and Takagi *et al.* (2013). F1 embryos were obtained from natural mating and *in vitro* fertilization using F0 transgenic females or males generated by REMI transgenesis.

Tail regeneration assay

Transgenic embryos possessing EGFP fluorescence in somite nuclei were screened at NF stage 41. Embryos were then anesthetized using MS-222 and approximately 1 mm of tail tip was amputated with a surgical scalpel. The embryos were incubated in 0.1× MMR at 18 °C for 4–5 days. Fluorescence images were taken every day.

ROS detection and inhibitor treatment

The compound 2′,7′-dichlorodihydrofluorescein diacetate (H2DCFDA; Life Technologies) was used to monitor ROS production in regenerating tail. Fluorescent carboxy-DCF was produced through ROS oxidation. Embryos were incubated with 25 μM H2DCFDA for 2 h before observation. For inhibitor treatment, a stock solution of 1 M APO (Sigma-Aldrich) was dissolved in DMSO (Sigma-Aldrich). DMSO (0.1%) was used as a solvent control. Embryos were incubated with 1 mM APO from 2 h before to 1 day after amputation. Five embryos were incubated with 5 mL of 0.1× MMR containing APO or DMSO in each well of a 6-well plate. Regeneration rate was evaluated according to previously reported criteria (regeneration index; Tseng *et al.* 2007).

Imaging

To track H3K9ac *in vivo* during embryogenesis and tail regeneration, Mintbody signal was observed using fluorescence stereomicroscopes (Leica MZ10F, M205FA and Olympus SZX16) and digital cameras (Nikon DS-Vi1, Olympus DP71, Leica DFC360 FX and Hamamatsu Photonics ORCA-FLASH 4.0).

Immunohistochemistry

Embryos were deeply anesthetized with 0.01%–0.05% MS-222 and fixed with 4% paraformaldehyde in phosphate-buffered saline (PBS) for 2 h at room temperature. Tissues were processed for paraffin embedding and then sectioned at 8 μm. Sections were deparaffinized, rehydrated and treated with 5 μg/mL proteinase K (Life Technologies) in Tris-buffered saline (TBS) for 25 min at RT. After the antigen retrieval step, sections were washed and blocked with Blocking One Histo (Nacalai Tesque) for 10 min at RT and incubated with rabbit anti-GFP antibody (ROCKLAND, diluted 1 : 400) for 1 h at 37 °C. After washing in TBS containing 0.1% Tween-20, sections were incubated with Alexa488-labeled secondary antibody (Life Technologies, diluted 1 : 400) and counterstained with DAPI or Hoechst 33342 (Life Technologies).

Acknowledgements

We thank Drs Haruki Ochi, Hiroshi Ochiai, Elizabeth Nakajima, Shigenori Nonaka and Atsushi Taniguchi and Ms. Haruka Akiyama for kindly providing plasmid, valuable comments, helps and frog maintenance. We also thank the National BioResource Project '*Xenopus tropicalis*' for providing plasmid, and the Spectrography and Bioimaging Facility and the NIBB Core Research Facilities for technical support. This work was supported by JSPS KAKENHI Grant Number 24510083 [Grant-in-Aid for Scientific Research (C)] and MEXT KAKENHI Grant Number 25124708 (Grant-in-Aid for Scientific Research on Innovative Areas) to K.T.S. This work was also supported by the NIBB Collaborative Research Programs (Grant no. 15-379 to K.T.S. and N.U. and 14-391 to T.E. and Y.K.).

References

Agricola, E., Verdone, L., Di Mauro, E. & Caserta, M. (2006) H4 acetylation does not replace H3 acetylation in chromatin

remodelling and transcription activation of Adr1-dependent genes. *Mol. Microbiol.* **62**, 1433–1446.

Beck, C.W., Christen, B., Barker, D. & Slack, J.M. (2006) Temporal requirement for bone morphogenetic proteins in regeneration of the tail and limb of *Xenopus* tadpoles. *Mech. Dev.* **123**, 674–688.

Beck, C.W., Christen, B. & Slack, J.M. (2003) Molecular pathways needed for regeneration of spinal cord and muscle in a vertebrate. *Dev. Cell* **5**, 429–439.

Beck, C.W., Izpisúa Belmonte, J.C. & Christen, B. (2009) Beyond early development: *Xenopus* as an emerging model for the study of regenerative mechanisms. *Dev. Dyn.* **238**, 1226–1248.

Chen, Y., Lin, G. & Slack, J.M. (2006) Control of muscle regeneration in the *Xenopus* tadpole tail by Pax7. *Development* **133**, 2303–2313.

Chen, Y., Love, N.R. & Amaya, E. (2014) Tadpole tail regeneration in *Xenopus*. *Biochem. Soc. Trans.* **42**, 617–623.

Choudhury, M., Park, P.H., Jackson, D. & Shukla, S.D. (2010) Evidence for the role of oxidative stress in the acetylation of histone H3 by ethanol in rat hepatocytes. *Alcohol* **44**, 531–540.

Dent, J.N. (1962) Limb regeneration in larvae and metamorphosing individuals of the South African clawed toad. *J. Morphol.* **110**, 61–77.

Endo, T., Tamura, K. & Ide, H. (2000) Analysis of gene expressions during *Xenopus* forelimb regeneration. *Dev. Biol.* **220**, 296–306.

Endo, T., Yokoyama, H., Tamura, K. & Ide, H. (1997) Shh expression in developing and regenerating limb buds of *Xenopus laevis*. *Dev. Dyn.* **209**, 227–232.

Endo, T., Yoshino, J., Kado, K. & Tochinai, S. (2007) Brain regeneration in anuran amphibians. *Dev. Growth Differ.* **49**, 121–129.

Fukazawa, T., Naora, Y., Kunieda, T. & Kubo, T. (2009) Suppression of the immune response potentiates tadpole tail regeneration during the refractory period. *Development* **136**, 2323–2327.

Gansen, A., Tóth, K., Schwarz, N. & Langowski, J. (2015) Opposing roles of H3- and H4-acetylation in the regulation of nucleosome structure—a FRET study. *Nucleic Acids Res.* **43**, 1433–1443.

Gargioli, C. & Slack, J.M. (2004) Cell lineage tracing during *Xenopus* tail regeneration. *Development* **131**, 2669–2679.

Gauron, C., Rampon, C., Bouzaffour, M., Ipendey, E., Teillon, J., Volovitch, M. & Vriz, S. (2013) Sustained production of ROS triggers compensatory proliferation and is required for regeneration to proceed. *Sci. Rep.* **3**, 2084.

Hamada, Y., Bando, T., Nakamura, T., Ishimaru, Y., Mito, T., Noji, S., Tomioka, K. & Ohuchi, H. (2015) Leg regeneration is epigenetically regulated by histone H3K27 methylation in the cricket *Gryllus bimaculatus*. *Development* **142**, 2916–2927.

Hamanaka, R.B., Glasauer, A., Hoover, P., Yang, S., Blatt, H., Mullen, A.R., Getsios, S., Gottardi, C.J., DeBerardinis, R.J., Lavker, R.M. & Chandel, N.S. (2013) Mitochondrial reactive oxygen species promote epidermal differentiation and hair follicle development. *Sci. Signal.* **6**, ra8.

Hayashi, S., Kawaguchi, A., Uchiyama, I., Kawasumi-Kita, A., Kobayashi, T., Nishide, H., Tsutsumi, R., Tsuru, K., Inoue, T., Ogino, H., Agata, K., Tamura, K. & Yokoyama, H. (2015) Epigenetic modification maintains intrinsic limb-cell identity in *Xenopus* limb bud regeneration. *Dev. Biol.* **406**, 271–282.

Johnson, A.D. & Krieg, P.A. (1994) pXeX, a vector for efficient expression of cloned sequences in *Xenopus* embryos. *Gene* **147**, 223–226.

Kraus, P., Fraidenraich, D. & Loomis, C.A. (2001) Some distal limb structures develop in mice lacking Sonic hedgehog signaling. *Mech. Dev.* **100**, 45–58.

Kroll, K.L. & Amaya, E. (1996) Transgenic *Xenopus* embryos from sperm nuclear transplantations reveal FGF signaling requirements during gastrulation. *Development* **122**, 3173–3183.

Kurdistani, S.K., Tavazoie, S. & Grunstein, M. (2004) Mapping global histone acetylation patterns to gene expression. *Cell* **117**, 721–733.

Lin, G., Chen, Y. & Slack, J.M. (2012) Transgenic analysis of signaling pathways required for *Xenopus* tadpole spinal cord and muscle regeneration. *Anat. Rec. (Hoboken)* **295**, 1532–1540.

Lin, G. & Slack, J.M. (2008) Requirement for Wnt and FGF signaling in *Xenopus* tadpole tail regeneration. *Dev. Biol.* **316**, 323–335.

Love, N.R., Chen, Y., Bonev, B., Gilchrist, M.J., Fairclough, L., Lea, R., Mohun, T.J., Paredes, R., Zeef, L.A. & Amaya, E. (2011) Genome-wide analysis of gene expression during *Xenopus tropicalis* tadpole tail regeneration. *BMC Dev. Biol.* **11**, 70.

Love, N.R., Chen, Y., Ishibashi, S., Kritsiligkou, P., Lea, R., Koh, Y., Gallop, J.L., Dorey, K. & Amaya, E. (2013) Amputation-induced reactive oxygen species are required for successful *Xenopus* tadpole tail regeneration. *Nat. Cell Biol.* **15**, 222–228.

Mochii, M., Taniguchi, Y. & Shikata, I. (2007) Tail regeneration in the *Xenopus* tadpole. *Dev. Growth Differ.* **49**, 155–161.

Nakade, S., Tsubota, T., Sakane, Y., Kume, S., Sakamoto, N., Obara, M., Daimon, T., Sezutsu, H., Yamamoto, T., Sakuma, T. & Suzuki, K.T. (2014) Microhomology-mediated end-joining-dependent integration of donor DNA in cells and animals using TALENs and CRISPR/Cas9. *Nat. Commun.* **5**, 5560.

Naora, Y., Hishida, Y., Fukazawa, T., Kunieda, T. & Kubo, T. (2013) Expression analysis of XPhyH-like during development and tail regeneration in *Xenopus* tadpoles: possible role of XPhyH-like expressing immune cells in impaired tail regenerative ability. *Biochem. Biophys. Res. Commun.* **431**, 152–157.

Nieuwkoop, P. & Faber, J. (1994) *Normal Table of Xenopus laevis* (Daudin). New York: Garland Publishing Inc.

Ogino, H., McConnell, W.B. & Grainger, R.M. (2006) High-throughput transgenesis in *Xenopus* using I-SceI meganuclease. *Nat. Protoc.* **1**, 1703–1710.

Pirotte, N., Stevens, A.S., Fraguas, S., Plusquin, M., Van Roten, A., Van Belleghem, F., Paesen, R., Ameloot, M., Cebrià, F., Artois, T. & Smeets, K. (2015) Reactive oxygen species in planarian regeneration: an upstream necessity for correct patterning and brain formation. *Oxid. Med. Cell. Longev.* **2015**, 392476.

Sakane, Y., Sakuma, T., Kashiwagi, K., Kashiwagi, A., Yamamoto, T. & Suzuki, K.T. (2014) Targeted mutagenesis of multiple and paralogous genes in *Xenopus laevis* using two pairs of transcription activator-like effector nucleases. *Dev. Growth Differ.* **56**, 108–114.

Sakuma, T., Ochiai, H., Kaneko, T., Mashimo, T., Tokumasu, D., Sakane, Y., Suzuki, K., Miyamoto, T., Sakamoto, N., Matsuura, S. & Yamamoto, T. (2013) Repeating pattern of non-RVD variations in DNA-binding modules enhances TALEN activity. *Sci. Rep.* **3**, 3379.

Sato, Y., Mukai, M., Ueda, J. *et al.* (2013) Genetically encoded system to track histone modification *in vivo*. *Sci. Rep.* **3**, 2436.

Satoh, A., Graham, G.M., Bryant, S.V. & Gardiner, D.M. (2008) Neurotrophic regulation of epidermal dedifferentiation during wound healing and limb regeneration in the axolotl (*Ambystoma mexicanum*). *Dev. Biol.* **319**, 321–335.

Slack, J.M., Lin, G. & Chen, Y. (2008) The *Xenopus* tadpole: a new model for regeneration research. *Cell. Mol. Life Sci.* **65**, 54–63.

St-Jacques, B., Dassule, H.R., Karavanova, I., Botchkarev, V.A., Li, J., Danielian, P.S., McMahon, J.A., Lewis, P.M., Paus, R. & McMahon, A.P. (1998) Sonic hedgehog signaling is essential for hair development. *Curr. Biol.* **8**, 1058–1068.

Stocum, D.L. (2011) The role of peripheral nerves in urodele limb regeneration. *Eur. J. Neurosci.* **34**, 908–916.

Suzuki, K.T., Isoyama, Y., Kashiwagi, K., Sakuma, T., Ochiai, H., Sakamoto, N., Furuno, N., Kashiwagi, A. & Yamamoto, T. (2013) High efficiency TALENs enable F0 functional analysis by targeted gene disruption in *Xenopus laevis* embryos. *Biol. Open* **2**, 448–452.

Suzuki, M., Yakushiji, N., Nakada, Y., Satoh, A., Ide, H. & Tamura, K. (2006) Limb regeneration in *Xenopus laevis* froglet. *ScientificWorldJournal* **6**(Suppl 1), 26–37.

Takagi, C., Sakamaki, K., Morita, H., Hara, Y., Suzuki, M., Kinoshita, N. & Ueno, N. (2013) Transgenic *Xenopus laevis* for live imaging in cell and developmental biology. *Dev. Growth Differ.* **55**, 422–433.

Taniguchi, Y., Watanabe, K. & Mochii, M. (2014) Notochord-derived hedgehog is essential for tail regeneration in *Xenopus* tadpole. *BMC Dev. Biol.* **14**, 27.

Taylor, A.J. & Beck, C.W. (2012) Histone deacetylases are required for amphibian tail and limb regeneration but not development. *Mech. Dev.* **129**, 208–218.

Tseng, A.S., Adams, D.S., Qiu, D., Koustubhan, P. & Levin, M. (2007) Apoptosis is required during early stages of tail regeneration in *Xenopus laevis*. *Dev. Biol.* **301**, 62–69.

Tseng, A.S., Carneiro, K., Lemire, J.M. & Levin, M. (2011) HDAC activity is required during *Xenopus* tail regeneration. *PLoS One* **6**, e26382.

Tseng, A.S. & Levin, M. (2008) Tail regeneration in *Xenopus laevis* as a model for understanding tissue repair. *J. Dent. Res.* **87**, 806–816.

Turner, D.L. & Weintraub, H. (1994) Expression of achaete-scute homolog 3 in *Xenopus* embryos converts ectodermal cells to a neural fate. *Genes Dev.* **8**, 1434–1447.

Yakushiji, N., Suzuki, M., Satoh, A., Sagai, T., Shiroishi, T., Kobayashi, H., Sasaki, H., Ide, H. & Tamura, K. (2007) Correlation between Shh expression and DNA methylation status of the limb-specific Shh enhancer region during limb regeneration in amphibians. *Dev. Biol.* **312**, 171–182.

Yakushiji, N., Yokoyama, H. & Tamura, K. (2009) Repatterning in amphibian limb regeneration: a model for study of genetic and epigenetic control of organ regeneration. *Semin. Cell Dev. Biol.* **20**, 565–574.

Yoshino, J. & Tochinai, S. (2004) Successful reconstitution of the non-regenerating adult telencephalon by cell transplantation in *Xenopus laevis*. *Dev. Growth Differ.* **46**, 523–534.

Received: 22 October 2015
Accepted: 13 January 2016

Supporting Information

Additional supporting information might/can be found in the supporting information tab for this article:

Figure S1 (A) A scheme for generating Mintbody transgenic *Xenopus laevis* using the microhomology-mediated end-joining (MMEJ)-dependent knock-in technique.

Figure S2 EGFP fluorescence pattern of EF1a:Mintbody F0 embryo during tail regeneration.

Figure S3 EGFP fluorescence pattern of CMV:Mintbody F1 embryos and tadpoles during tail regeneration.

Figure S4 Enhancement of Mintbody signal by TSA treatment in F1 embryos.

Figure S5 Time-course observation of CMV:Mintbody F1 embryo during tail regeneration.

Figure S6 Regeneration rate following treatment with various concentrations of APO.

Table S1 Primers for inverse PCR to add modified *xl-tyr*TALEN recognition site

Table S2 Increase of H3K9ac-Mintbody signal in the regenerating notochord and wound epithelium in DMSO- and APO-treated embryos